JJCO Japanese Journal of Clinical Oncology

Jpn J Clin Oncol 2014;44(9)826–834
doi:10.1093/jjco/hyu079
Advance Access Publication 10 June 2014

A New Middle-range Diameter Bronchoscope with Large Channel for Transbronchial Sampling of Peripheral Pulmonary Lesions

Shinji Sasada*, Takehiro Izumo, Christine Chavez, Yuji Matsumoto and Takaaki Tsuchida

Department of Endoscopy, Respiratory Endoscopy Division, National Cancer Center Hospital, Tokyo, Japan

*For reprints and all correspondence: Shinji Sasada, Department of Endoscopy, Respiratory Endoscopy Division, National Cancer Center Hospital, 5-1-1 Tsukiji, Chuo-ku, Tokyo, 104-0054 Japan. E-mail: sasastaf@hotmail.co.jp

Received March 31, 2014; accepted May 15, 2014

Objective: Although the diagnostic yield of guided bronchoscopy for peripheral pulmonary lesions has improved to 70%, it is still low compared with transthoracic needle aspiration. We produced a new bronchoscope with middle-range diameter and large channel (BF-Y0053, Olympus, Japan), and evaluated its diagnostic efficacy for peripheral pulmonary lesions.
Methods: This was a retrospective study on 70 consecutive patients with peripheral pulmonary lesions who underwent diagnostic bronchoscopy using BF-Y0053 combined with endobronchial ultrasound with a guide sheath at the National Cancer Center Hospital from September 2013 to November 2013. Diagnostic performance of the procedure was analyzed and compared among three groups of peripheral pulmonary lesions: 'peripheral-small' lesions ($\leq$30 mm and adjacent to visceral pleura), 'central-small' lesions ($\leq$30 mm and not adjacent to the visceral pleura), and 'large' lesions ($>$30 mm).
Results: Sixty (85.7%) patients had malignant diseases. Diagnosis was established by bronchoscopy in 61 of 70 patients (87.1%); the respective yields for 'central-small' and 'large' lesions were significantly higher than that for 'peripheral-small' lesions (96.3%, 94.4%, 72%, $P = 0.0026$). This diagnostic accuracy was achieved regardless of other clinical and procedural factors such as, lesion size, feature ground glass opacity (or solid), endobronchial ultrasound-probe location (within or outside) or operator skill. There were no major post-procedural complications.
Conclusions: A new middle-range diameter bronchoscope with large channel combined with endobronchial ultrasound with a guide sheath can enhance the efficacy of transbronchial sampling to its maximal potential to diagnose peripheral pulmonary lesions safely and accurately, particularly for patients who have tumors away from the visceral pleura.

Key words: middle-range diameter bronchoscope with large channel – endobronchial ultrasonography with a guide sheath – transbronchial biopsy – peripheral pulmonary lesions

INTRODUCTION

Lung cancer is one of the most common cancer-related deaths in the USA, Europe and Japan (1–3). Current guidelines in the management of lung cancer recommend bronchoscopy as one of the non-surgical procedures with a more favorable safety profile for tissue diagnosis of peripheral pulmonary lesions (PPLs) (4). According to a recent meta-analysis, the yield of guided bronchoscopy using new techniques such as, virtual bronchoscopic navigation (VBN) (5), endobronchial ultrasonography with a guide sheath (EBUS-GS) (6,7) and ultrathin fiber was ~70% (8). Although this has improved over the last 10 years, it is still low compared with transthoracic needle aspiration (TTNA) (4). Hence, most chest physicians worldwide still choose TTNA despite reports on higher risk for complications such as, pneumothorax, air embolism and tumor seeding (9,10).

To bridge the gap that curtails achievement of a similar diagnostic yield to TTNA, several technicalities surrounding transbronchial biopsy (TBB) need to be addressed. The most important factor that has been reported in the literature is localization of the target PPL with the aid of computed tomography (CT), fluoroscopy, ultrathin bronchoscopy, EBUS and VBN but results on diagnostic yields were still relatively low compared with TTNA (11–13). Another issue is procurement of adequate amounts of tissue. In general, a definitive or molecular diagnosis is difficult to confirm in small samples, but these matters are not discussed enough. In the recently published guidelines by the IASLC, selection of appropriate molecular targeted drugs for all patients with advanced lung adenocarcinoma entails a search for epidermal growth factor receptor mutation and echinoderm microtubule-associated protein-like 4 gene and the anaplastic lymphoma kinase gene fusion (14). To facilitate molecular analysis for several genes, sufficient amount of tissue samples is required (15). An optimal transbronchial biopsy technique would constitute precise localization of the target lesion and acquisition of an enough amount of biopsy specimen.

Current available bronchoscopes and GSs are mainly divided into two varieties: one has thin outer diameter with a small working channel (e.g. BF-P260F, Olympus) and small size devices (e.g. K-201, small size GS, 1.95 mm in diameter, Olympus), the other has thick outer diameter with a large working channel (e.g. BF-1T260, Olympus) and large size devices (e.g. K-203, large size GS, 2.55 mm in diameter, Olympus). These differ in terms of ability to approach a lesion, size of tissue samples that can be obtained and ease of handling. To address these concerns of achieving an optimal TBB technique, we produced a new bronchoscope that has middle-range outer diameter with a large working channel through which any size of radial EBUS probe and large size GS kit can be inserted. We hypothesize that these design specifications would satisfy the requirements of increasing the diagnostic yield for PPLs. In this study, we evaluated the diagnostic efficacy of this new bronchoscope combined with EBUS-GS for TBB of PPLs.

PATIENTS AND METHODS

Study Design and Patients

From September 2013 to November 2013, 107 consecutive patients with PPLs underwent diagnostic bronchoscopy EBUS-GS transbronchial sampling at the National Cancer Center Hospital; in 70 of these patients, a new middle-range bronchoscope with large channel was used. The choice to use this new bronchoscope was judged by the operator, depending on the difficulty in approaching the target lesion based on CT scan image. Examples of difficult to reach lesions were those with no apparent bronchus sign, with ground glass opacity, and located in the upper lobe, segment 6, and the like. PPL was defined as an abnormal growth surrounded by lung parenchyma and with no evidence of endobronchial involvement. Definitive diagnoses of all lesions were proven by transbronchial biopsy or surgical resection after bronchoscopy. Written informed consent was procured from all patients. A retrospective review of electronic medical records was performed. This study was evaluated by the National Cancer Center Institutional Review Board.

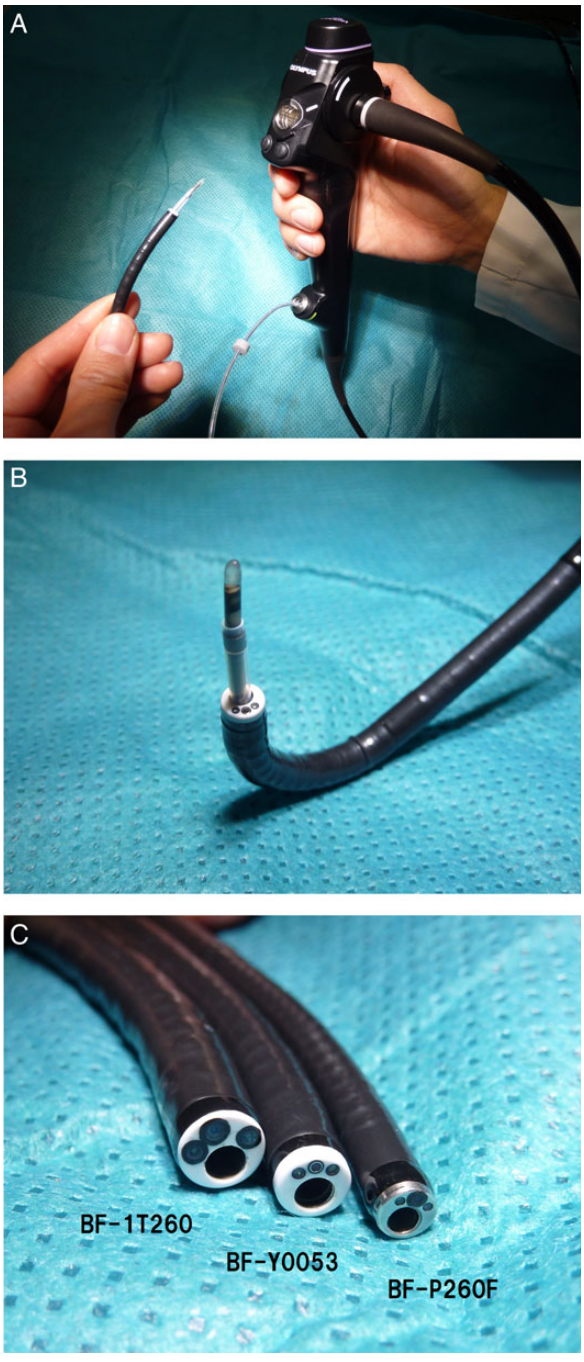

Figure 1. (A) An image of middle-range diameter bronchoscope with large channel (BF-Y0053, Olympus). (B) A large guide sheath kit (K203, Olympus), with radial endobronchial ultrasound (EBUS) probe can be through the working channel of BF-Y0053. (C) Comparison of the bronchoscope tips, BF-1T260 (left, 5.9 mm outer diameter and 2.8 mm working channel), BF-Y0053 (center, 5.1 and 2.6 mm, respectively) and BF-P260F (right, 4.0 and 2.0 mm, respectively). The tip of BF-Y0053 is narrow in shape.

New Middle-range Diameter Bronchoscope with Large Channel

The new bronchoscope (BF-Y0053; Olympus) had a 5.1 mm outer diameter and 2.6 mm working channel diameter through which a large GS kit (K-203) can be inserted (Fig. 1A). The shape of the handle and degree of angulation (180° flexion, 130° extension) of BF-Y0053 are similar to currently available bronchoscopes (Fig. 1B), and the size of scope tip is middle-range between BF-1T260 (5.9 mm outer diameter and 2.8 mm working channel) and BF-P260F (4.0 mm outer diameter and 2.0 mm working channel) (Fig. 1C).

EBUS-GS Transbronchial Sampling Procedure

For all cases, the bronchial path to the target lesion was planned using 1.0 mm sequential axial CT scan slices. CT was performed using a multi-detector CT scanner (Aquilion PRIME®; Toshiba; Tokyo, Japan). Helical volume data sets were acquired during single breath-hold inhalations. VBN was reconstructed from helical CT data and transferred to a work station (Ziostation2®; Ziosoft Inc., Tokyo, Japan).

Each patient received local anesthesia of the upper respiratory tract using 4% lidocaine, pre-medication of 17.5 mg pethidine hydrochloride, and sprayed using 2% lidocaine during bronchoscopy under conscious sedation with 3–5 mg midazolam. Flexible bronchoscopy was done using BF-Y0053 in combination with a radial ultrasound probe (UM-S20–20R; Olympus) and large size GS kit (K203). Following the VBN made by Ziostation2®, BF-Y0053 was wedged as deeply as possible into the target bronchus under direct vision. The EBUS probe, together with the GS, was inserted through the working channel and advanced to reach the PPL under fluoroscopy guidance (VersiFlex VISTA®, Hitachi, Japan). After localizing the lesion by EBUS, the probe was removed while the guide sheath was kept in place. If the target lesion was not detected by EBUS, the probe was manipulated under fluoroscopy guidance until an acoustic signal was generated. A 1.8 mm biopsy forceps (FB-231D; Olympus) and a bronchial brush (BC-2020-2010; Olympus) were alternately inserted

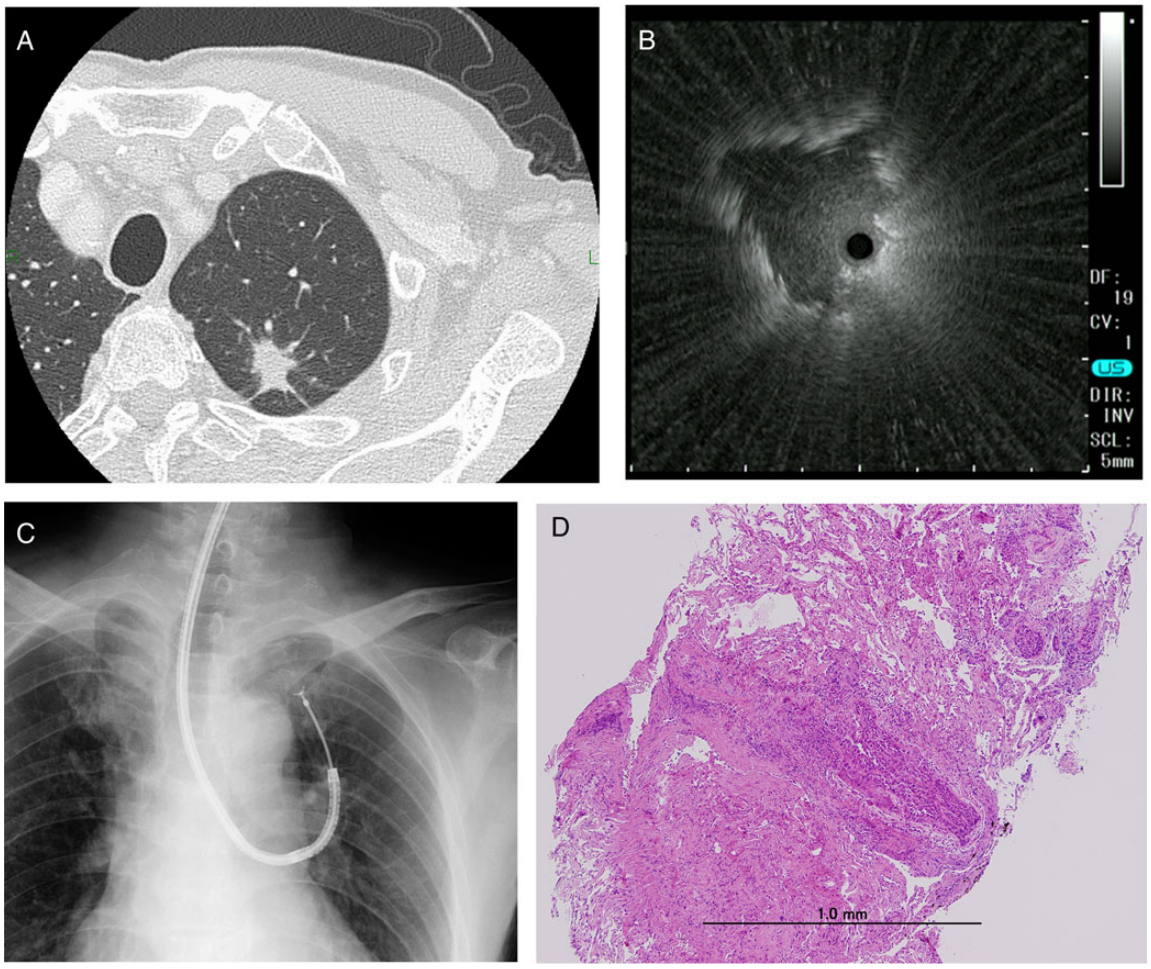

Figure 2. A case of 72-year-old man who was admitted to our hospital because of chest abnormal shadow. (A) Computed tomography (CT) scan shows a solid tumor measuring 18 mm in the largest diameter and located in the left S1+2, classified as 'central-small'. (B) The EBUS probe was advanced into the B1+2a bronchus following virtual bronchoscopic navigation, demonstrating low-echoic nodule located adjacent to. (C) Fluoroscopy imaging during endobronchial ultrasound with a guide sheath (EBUS-GS) procedure. (D) Histopathological specimen from the transbronchial biopsy showed squamous cell carcinoma. (hematoxylin–eosin stain, ×40)

through the GS to get specimens for pathology examinations (Fig. 2). When the EBUS image showed adjacent to or invisible findings and sufficient materials could not be obtained, transbronchial needle aspiration through a large GS (GS-TBNA) using a 21G aspiration needle (NA-1C-1, Olympus) was done (Fig. 3) (16).

In all of the 70 cases, samples were successfully obtained by brush, forceps and/or GS-TBNA. Each histology and cytology specimen was interpreted separately by an experienced pathologist. The final diagnoses were established by pathologic evidence from bronchoscopic or surgical biopsy, microbiological analysis or clinical follow-up. Bronchoscopy was considered as diagnostic when pathology examination of tissue samples were positive for malignancy and/or cytology samples were Class IV or V. For the EBUS-GS guided samples that were diagnosed as inflammatory change, follow-up CT imaging was done after at least 3 months. Lesions that resolved were designated as benign. Bronchoscopy procedures were performed by two staff members or seven pulmonary residents who were directly supervised by the experts in attendance.

Study Variables and Statistical Analysis

Data on demographics, radiological characteristics, bronchoscopy device and findings and final diagnoses were collected. PPL was measured in the largest diameter on the axial plane CT image. Based on a previous paper (17), CT scan characteristics were classified as GGO (pure or part-solid) or solid. Data gathered from the bronchoscopy procedure were EBUS-probe location, number of tissue samples and procedure time (from vocal cord insertion to removal of the guide sheath). Lobar location was recorded as upper, middle/lingula and lower. Lesion area was designated as 'peripheral-small' if the lesion was $\leq$30 mm and adjacent to the visceral pleura, or if the nodule was very small (solid $\leq$10 mm or pure GGO $\leq$ 15 mm) and located in the outer half of the hemithorax, 'central-small' if the lesion was $\leq$30 mm and not

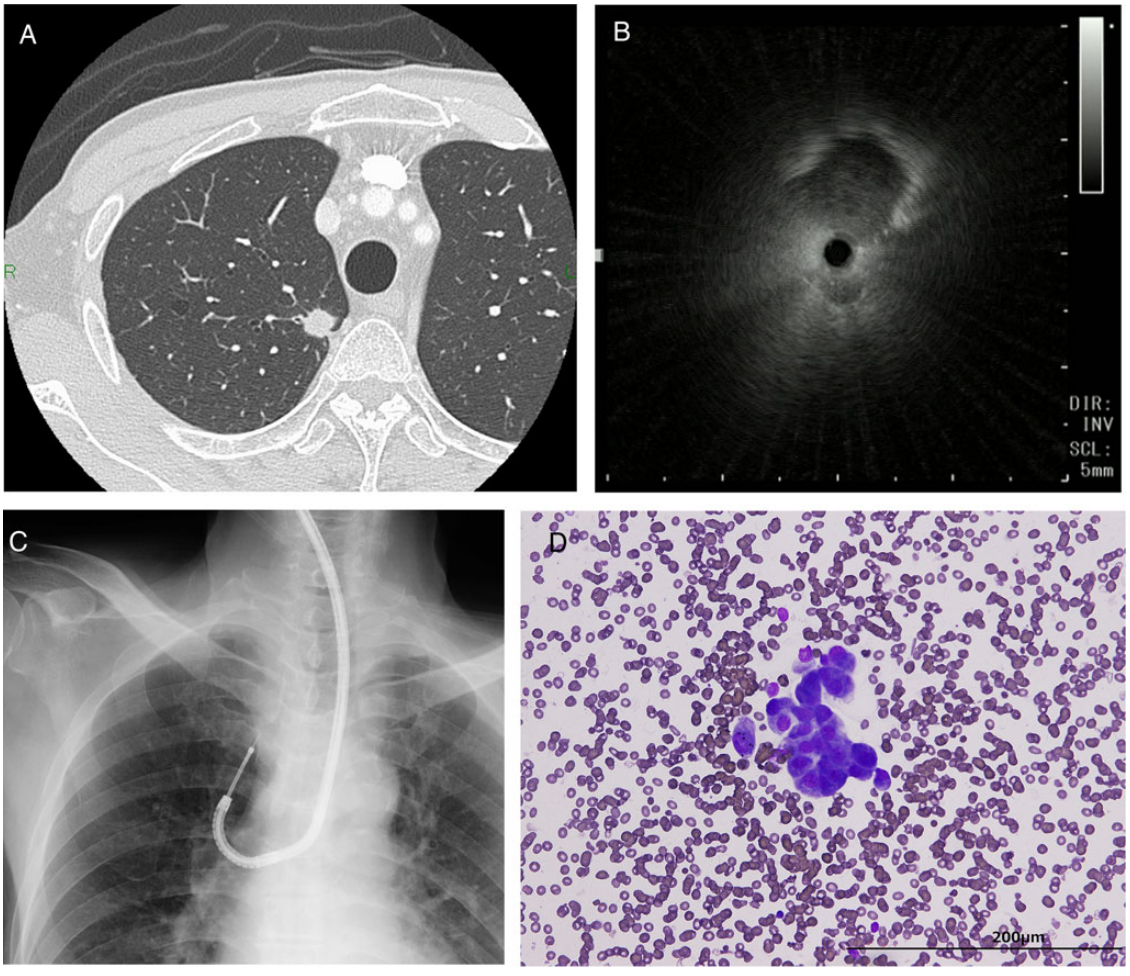

Figure 3. A case of 75-year-old man with chest abnormal shadow in right upper lobe. (A) CT scan shows 9 mm solid tumor adjacent to visceral pleura, classified as 'peripheral-small'. (B) The EBUS image through right B1a reveals low-echoic lesion located adjacent to. (C) Fluoroscopy imaging during transbronchial needle aspiration through a guide sheath (GS-TBNA) procedure. (D) Cytological specimen from GS-TBNA shows adenocarcinoma. (papanicalou stain, ×100)

adjacent to the visceral pleura, and 'large' if the lesion was >30 mm. In this study, we classified the very small lesions (solid ≤10 mm or pure GGO ≤ 15 mm) into 'peripheral-small' group. The reason was that the approach to very small lesions was nearly similar to that of lesions adjacent to the visceral pleura.

Descriptive statistics was presented as frequency, percentage and mean ± standard deviation (SD). We investigated the factors affecting diagnostic yield using Fisher's Exact Test. *P* values were two-sided and a level of ≤0.05 was considered statistically significant. Statistical analyses were performed with EZR® (Saitama Medical Center, Jichi Medical University; http://www.jichi.ac.jp/saitama-sct/SaitamaHP.files/statmed.html; Kanda), a graphical user interface for R (The R Foundation for Statistical Computing, Vienna, Austria, Ver. 2. 13.0) and a modified version of R commander (Ver. 1.8-4).

RESULTS

A summary of the baseline characteristics of the patients are shown in Table 1. The study population included 70 patients, 43 male and 27 female, age 67.4 ± 9.1 years, who had peripheral pulmonary lesions that measured 25.5 ± 13.1 mm and

Table 1. Baseline characteristics of patients with peripheral pulmonary lesions ($N = 70$)

Variables	Values, mean ± SD			
	All lesions	Peripheral-small	Central-small	Large
Number of subjects (%)	70	25 (35.7)	27 (38.5)	18 (25.7)
Age (years)	67.4 ± 9.1	67.8 ± 7.3	67.7 ± 9.4	66.6 ± 11.2
Gender, no. (%)				
Male	43 (61.4)	14 (56.0)	18 (66.7)	11 (61.1)
Female	27 (38.6)	11 (44.0)	9 (33.3)	7 (38.9)
Lobar location, no. (%)				
Upper	36 (51.4)	11 (44.0)	16 (59.3)	9 (50.0)
Middle or lingular	7 (10.0)	2 (8.0)	3 (11.1)	2 (11.1)
Lower	27 (38.6)	12 (48.0)	8 (29.6)	7 (28.9)
Lesion size (mm)	25.5 ± 13.1	18.2 ± 6.8	19.8 ± 4.2	44.1 ± 10.4
Feature, no. (%)				
Pure GGO	6 (8.6)	2 (8.0)	4 (14.8)	0
Part-solid GGO	14 (20.0)	8 (32.0)	3 (11.1)	3 (16.7)
Solid nodule	50 (71.4)	15 (60.0)	20 (74.1)	15 (83.3)
EBUS-probe location, no. (%)				
Within-solid	34 (48.6)	8 (32.0)	15 (55.6)	11 (61.1)
Within-Blizzard sign	5 (7.1)	4 (16.0)	1 (3.7)	0
Adjacent to	22 (31.4)	6 (24.0)	9 (33.3)	7 (38.9)
Not visualized	9 (12.9)	7 (28.0)	2 (7.4)	0
Primary disease, no. (%)				
Malignant	60 (85.7)	20 (80.0)	23 (85.2)	17 (94.4)
Benign	10 (14.3)	5 (20.0)	4 (14.8)	1 (5.6)
Devices, no. (%)				
EBUS-GS	64 (91.4)	24 (96.0)	26 (96.3)	14 (77.8)
EBUS-GS and TBNA	6 (8.6)	1 (1.4)	1 (3.7)	4 (22.2)
Procedure time (min)	23.8 ± 8.1	24.8 ± 8.1	22.2 ± 9.4	24.6 ± 8.3
Biopsy number (pieces)	4.9 ± 1.4	4.6 ± 1.8	4.9 ± 0.9	5.5 ± 1.4
Operator, no. (%)				
Staff	10 (14.3)	5 (20.0)	2 (7.4)	3 (16.7)
Resident	60 (85.7)	20 (80.0)	25 (92.6)	15 (83.3)

GGO, ground glass opacity; SD, standard deviation; EBUS, endobronchial ultrasonography; GS, guide sheath; TBNA, transbronchial needle aspiration.

Table 2. Univariate analysis of the factors affecting diagnostic yield for peripheral pulmonary lesions ($N = 70$)

Variables	Univariate analysis, diagnostic no./total no. (%)	
	All lesions	*P* value
Overall	61/70 (87.1)	
Age (years)		
≤67	29/34 (86.5)	0.731
>67	32/36 (87.9)	
Gender		
Male	37/43 (86)	1
Female	24/27 (88.8)	
Lobar location		
Upper	30/36 (83.3)	0.61
Middle or lingular	6/7 (85.7)	
Lower	25/27 (92.5)	
Lesion size (mm)		
≤20	26/32 (81.3)	0.438
>20, ≤30	18/20 (90)	
>30	17/18 (94.4)	
Feature		
Pure GGO	4/6 (66.6)	0.322
Part-solid GGO	13/14 (92.8)	
Solid nodule	44/50 (88)	
EBUS-probe location[a]		
Within	35/39 (89.7)	0.496
Outside	26/31 (83.9)	
Primary disease		
Malignant	53/60 (88.3)	0.475
Benign	8/10 (80)	
Devices		
EBUS-GS	55/64 (85.9)	1
EBUS-GS and TBNA	6/6 (100)	
Procedure time (min)		
≤23	33/37 (87.8)	0.726
>23	28/33 (86.2)	
Biopsy number (pieces)		
<5	13/17 (76.5)	0.206
≥5	48/53 (90.6)	
Operator		
Staff	10/10 (100)	0.592
Resident	51/60 (85)	

TBNA, transbronchial needle aspiration.
[a]Outside include adjacent to and not visualized.

Table 3. Univariate analysis of the factors affecting diagnostic yield between three different lesion areas ($N = 70$)

Variables	Univariate analysis, diagnostic no./total no. (%)			
	Peripheral-small	Central-small	Large	*P* value
Overall	18/25 (72)	26/27 (96.3)	17/18 (94.4)	0.021
Lobar location				
Upper	7/11 (63.6)	15/16 (93.8)	8/9 (88.9)	0.125
Middle or lingular	1/2 (50)	3/3 (100)	2/2 (100)	0.4
Lower	10/12 (83.3)	8/8 (100)	7/7 (100)	0.49
Feature				
Pure GGO	0/2 (0)	4/4 (100)	0	0.067
Part-solid GGO	7/8 (87.5)	3/3 (100)	3/3 (100)	1
Solid nodule	11/15 (73.3)	19/20 (95)	14/15 (93.3)	0.141
Lesion size (mm)				
≤20	14/20 (70)	23/23 (100)	0	0.018
>20	8/9 (88.9)	10/11 (90.9)	17/18 (94.4)	1
EBUS-probe location[a]				
Within	9/12 (75)	16/16 (100)	10/11 (90.1)	0.067
Outside	9/13 (69.2)	10/11 (90.1)	7/7 (100)	0.327
Operator				
Staff	5/5 (100)	2/2 (100)	3/3 (100)	1
Resident	13/20 (65)	24/25 (96)	14/15 (93.3)	0.015

[a]Outside include adjacent to and not visualized.

that were most commonly located in the upper lobe; 20 (28.6%) were GGO in character. Sixty-one (87.1%) of the PPLs were visualized by EBUS and subsequently underwent transbronchial sampling through a guide sheath. Sixty (85.7%) patients had malignant diseases. Six (15%) lesions underwent GS-TBNA. Mean procedure time was 23.8 ± 8.1 min, and mean number of histologic specimens obtained was 4.9 ± 1.4 per procedure. Sixty procedures (85.7%) were performed by residents. There was no difference between the sizes of 'peripheral-small' lesions and 'central-small' lesions (18.2 ± 6.8 mm, 19.8 ± 4.2 mm, respectively).

Bronchoscopy using BF-Y0053 combined with EBUS-GS was diagnostic in 61 of 70 patients (87.1%). Clinical and procedural parameters such as, lobar location, lesion size, feature (GGO or solid), devices, EBUS-probe location, primary disease, sampling number and operator skill did not affect the diagnostic yield (Table 2).

A comparison among the groups of lesion area, 'peripheral-small', 'central-small' and 'large' are shown in Table 3. Diagnostic yields for 'central-small' lesions (96.3%) and 'large' lesions (94.4%) were significantly higher than that of 'peripheral-small' lesions (72%) ($P = 0.021$). For tumors ≤20 mm in size, 'central-small' lesions were all successfully diagnosed and had significantly higher yield than that of 'peripheral-small' lesions ($P = 0.018$). There were four pure GGO lesions in 'central-small' group and all of these were diagnosed successfully by bronchoscopy. In contrast, the diagnostic yield for 'peripheral-small' lesions that were handled by residents was significantly lower than that of other lesions ($P = 0.015$).

Table 4. Final diagnosis in three different location areas ($N = 70$)

Pathologic diagnosis	Patients (final diagnosis), no.		
	Peripheral-small ($N = 25$)	Central-small ($N = 27$)	Large ($N = 18$)
Malignant			
Primary lung cancer	14	23	16
Adenocarcinoma	11	16	8
Squamous cell carcinoma	1	4	3
NSCLC	0	1	4
Small cell carcinoma	0	1	0
Metastatic carcinoma	2 (1 Bladder cancer, 1 breast cancer)	1 (1 Uterine cancer)	1 (1 Rectal cancer)
Benign			
Non-specific inflammation	4	0	0
Granuloma	0	2 (2 Unspecified)	1 (1 Unspecified)
Anthracosis	0	1	0
Non-diagnostic			
Non-representative results	7 (6 Lung cancers, 1 non-specific inflammation)	1 (1 Non-specific inflammation)	1 (1 Lung cancer)

NSCLC, non-small cell lung cancer.

Table 4 shows the pathological results of EBUS-GS transbronchial sampling and the distribution of the final diagnoses among the three groups of location-size. Final diagnosis in the majority of patients was adenocarcinoma; all four metastatic lesions were successfully diagnosed by bronchoscopy. Bronchoscopy was non-diagnostic in nine lesions; these included three lesions that had atypical cells suspicious for malignancy on cytology and three nodules that were visible on EBUS but yielded insufficient biopsy and brushing samples. Of these non-diagnostic cases by bronchoscopy, seven lesions were established to be primary lung cancers (four adenocarcinomas, two squamous cell carcinomas and one NSCLC) by surgical biopsy. The remaining two lesions (one solid and one part-solid GGO) decreased in size on follow-up and were designated as inflammation. Diagnosis was established by histopathology in 53 lesions (75.7%) and by cytology in 44 lesions (62.8%).

Among the 70 procedures, pneumothorax occurred in two patients and one of them required chest tube insertion. Major complications such as massive bleeding or air embolism were not observed.

DISCUSSION

In recent years, the diagnostic yield of bronchoscopy for PPL has been reported to be 60–80% (7,13,18), these results are significantly lower than the >90% yield of TTNA (19), making the latter a procedure of choice in most countries. In this study, the use of BF-Y0053 combined with EBUS-GS achieved an 87.1% diagnostic yield of TBB for PPLs. In most related study using thin bronchoscope with small GS kit, the diagnostic yield was usually lower than the EBUS visualization rate (5), but our results showed similar diagnostic yield and EBUS visualization rate. We consider that having sufficient amount of samples obtained by a large GS kit and GS-TBNA may have contributed to the results (12). Our data also suggest that the use of BF-Y0053 combined with EBUS-GS may be advantageous regardless of lobar location, lesion size, feature (GGO or solid), EBUS-probe location, sampling number and operator skill. Additionally, the mean procedure time ~24 min is reasonable for daily practice. Pneumothorax was occurred in two cases (2.8%) of non-GS-TBNA group. There were no major complications such as massive bleeding or other events.

Diagnostic performance of bronchoscopy for PPL had been reported to be dependent on the technical ability of inserting biopsy instruments into a PPL, which is influenced by distance from the hilum to the lesion (20). In this study, we added size as a contributing factor to this anatomic difficulty and divided the PPLs into three groups: 'peripheral-small', 'central-small' and 'large'. Our data show a 96% yield for 'central-small' lesions, demonstrating that EBUS-GS transbronchial sampling using BF-Y0053 has extremely high diagnostic ability even for small PPLs so long as the location is away from the visceral pleura. On the other hand, the diagnostic yield using Y0053 in 'peripheral-small' lesions was 72%, which is comparable to previously published data on diagnostic bronchoscopy (21). To improve the diagnostic yield, a combination of thin bronchoscope (BF-P260F) and small size GS kit (K-201) can be selected. However, the amount of collected sample is often small and inadequate for definitive pathologic diagnosis when obtained by a thin device (22). Of course, TTNA or video-assisted thoracoscopic surgery are also options in these cases.

Peripheral pulmonary lesions that cannot be precisely detected by EBUS (adjacent to or not visualized) were reported to be significant predictors of low diagnostic yield (6). To address this issue, we performed additional GS-TBNA on six lesions that cannot be sampled by usual TBB, and all of them were diagnostic. We deduce that sampling from difficult-to-approach lesions was possible by GS-TBNA because the needle can penetrate through a compressed bronchus.

The outer diameter of BF-Y0053 is in the middle-range of 5.1 mm. Although this size is larger than that of BF-P260F, we observed that using the BF-Y0053 allowed farther insertion up to the fourth–fifth generation bronchial segments and visualization of the lumen of the succeeding branches. We consider that the narrowed tip of the BF-Y0053 facilitated dilation of the bronchial lumen, making it possible to advance and wedge the scope closer to the target during TBB. This feature could have helped overcome the

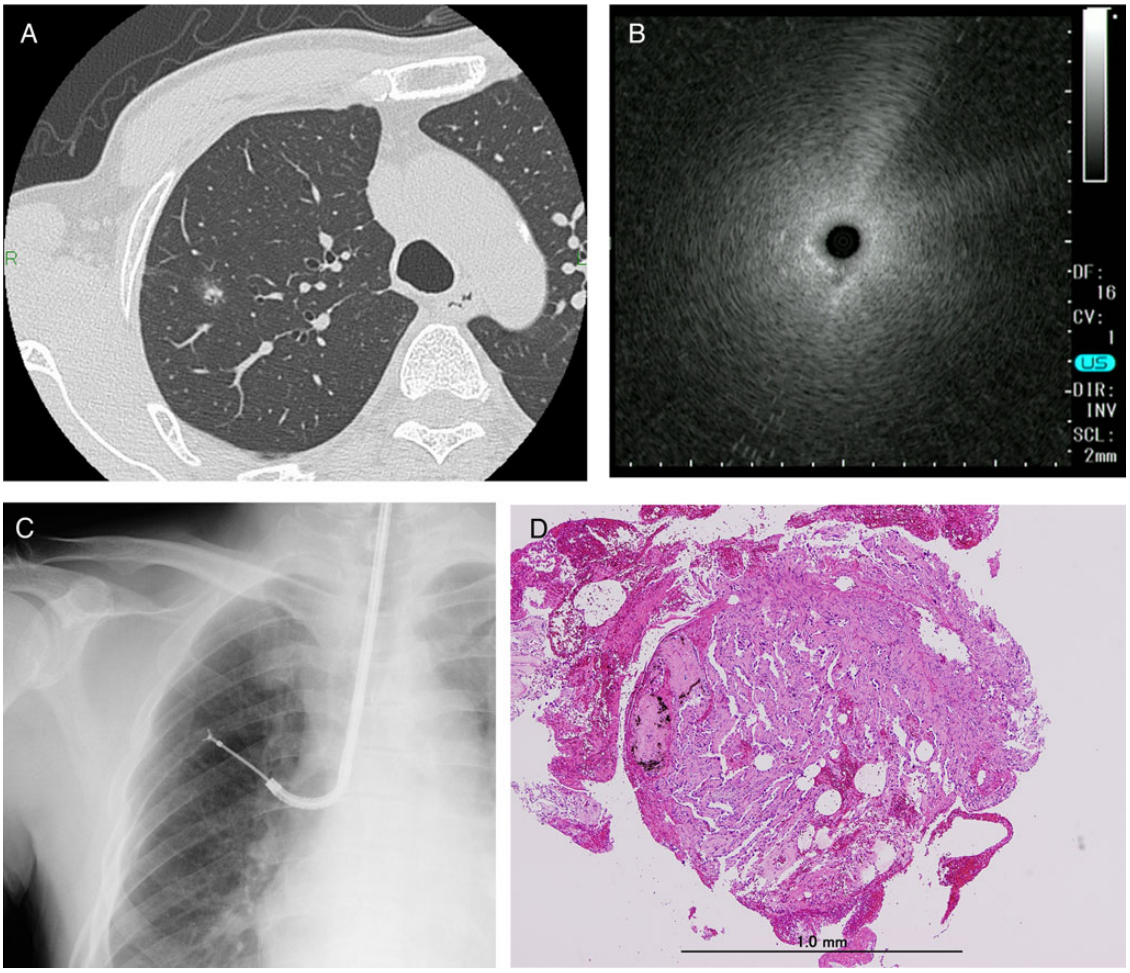

Figure 4. A case of 66-year-old man with chest abnormal shadow in right upper lobe. (A) CT scan shows 12 mm part solid ground glass opacity away from visceral pleura, classified as 'central-small'. (B) The EBUS image through right B2b reveals Blizzard sign, which shows coarse hyperechoic signals. (C) Fluoroscopy imaging during EBUS-GS procedure. (D) Histopathological specimen from EBUS-GS shows adenocarcinoma with lepidic growth. (hematoxylin–eosin stain, ×40)

technical and anatomic difficulty of accurate sampling from a PPL.

The value of diagnostic bronchoscopy for GGO had been recognized to be difficult because of poor visualization by fluoroscopy and EBUS (23). We previously reported Blizzard sign, which is coarse hyperechoic signals, as a specific EBUS image for GGO lesions (22). In our present study, we used this sign as an indication of EBUS-GS localization of five GGO lesions prior to TBB and in 90% of these, the diagnosis was successfully established (Fig. 4).

One limitation of this study is the retrospective, non-randomized design. Further prospective study designs are warranted.

In conclusion, a new middle-range diameter bronchoscope with large channel combined with EBUS-GS can enhance the diagnostic efficacy of the emerging procedure, transbronchial sampling of PPLs. This technical improvement has a great potential for most of patients with PPLs who need to be diagnosed safely and accurately, especially if the tumor is away from the visceral pleura.

Ethical Issues

This study was approved by the hospital's Institutional Review Board and Ethics Committee; informed consent was sought from the patients.

Acknowledgements

We thank Koji Tsuta for supporting the pathological examinations.

Funding

This work was supported by The National Cancer Center Research and Development Fund (25-A-12).

Conflict of interest statement

None declared.

References

1. Matsuda T, Marugame T, Kamo K, et al. Cancer incidence and incidence rates in Japan in 2006: based on data from 15 population-based cancer registries in the monitoring of cancer incidence in Japan (MCIJ) project. *Jpn J Clin Oncol* 2012;42:139–47.
2. Siegel R, Naishadham D, Jemal A. Cancer statistics, 2013. *CA Cancer J Clin* 2013;63:11–30.
3. Gatta G, Zigon G, Capocaccia, et al. Survival of European children and young adults with cancer diagnosed 1995–2002. *Eur J Cancer* 2009;45:992–1005.
4. Detterbeck FC, Lewis SZ, Diekemper R, et al. Executive summary: diagnosis and management of lung cancer, 3rd: American college of chest physicians evidence-based clinical practice guidelines. *Chest* 2013;143:7S–37S.
5. Ishida T, Asano F, Yamazaki K, et al. Virtual bronchoscopic navigation combined with endobronchial ultrasound to diagnose small peripheral pulmonary lesions: A randomised trial. *Thorax* 2007;131:549–53.
6. Kurimoto N, Miyazawa T, Okimasa S, et al. Endobronchial ultrasonography using a guide sheath increases the ability to diagnose peripheral pulmonary lesions endoscopically. *Chest* 2004; 126:959–65.
7. Kikuchi E, Yamazaki K, Sukoh N, et al. Endobronchial ultrasonography with guide-sheath for peripheral pulmonary lesions. *Eur Respir J* 2004;24:533–7.
8. Wang Memoli JS, Nietert PJ, Silvestri GA, et al. Meta-analysis of guided bronchoscopy for the evaluation of the pulmonary nodule. *Chest* 2012;142:385–93.
9. Wiener RS, Schwarts LM, Woloshin S, et al. Population-based risk for complications after transthoracic needle lung biopsy of a pulmonary nodule: an analysis of discharge records. *Ann Intern Med* 2011;155:137–44.
10. Tomiyama N, Yasuhara Y, Nakajima Y, et al. CT-guided needle biopsy of lung lesions: a survey of severe complication based on 9783 biopsies in Japan. *Eur J Radiol* 2006;59:60–4.
11. Fielding DI, Chia C, Nguyen P, et al. Prospective randomised trial of endobronchial ultrasound-guide sheath versus computed tomography-guided percutaneous core biopsies for peripheral lung lesions. *Intern Med J* 2012;42:894–900.
12. Shinagawa N, Yamazaki K, Onodera Y, et al. CT-guided transbronchial biopsy using an ultrathin bronchoscope with virtual bronchoscopic navigation. *Chest* 2004;125:1138–43.
13. Asano F, Shinagawa N, Ishida T, et al. Virtual bronchoscopic navigation combined with ultrathin bronchoscopy. A randomized clinical trial. *Am J Respir Crit Care Med* 2013;188:327–33.
14. Lindeman NI, Cagle PT, Beasley MB, et al. Molecular testing guideline for selection of lung cancer patients for EGFR and ALK tyrosine kinase inhibitors: guideline from the College of American Pathologists, International Association for the Study of Lung Cancer, and Association for Molecular Pathology. *J Thorac Oncol* 2013;8:823–59.
15. Nakajima T, Yasufuku K. How to do it-optimal methodology for multidirectional analysis of endobronchial ultrasound-guided transbronchial needle aspiration samples. *J Thorac Oncol* 2011;6:203–6.
16. Takai M, Izumo T, Chavez C, et al. Transbronchial needle aspiration through a guide sheath with endobronchial ultrasonography (GS-TBNA) for peripheral pulmonary lesions. *Ann Thorac Cardiovasc Surg* 2014;20:19–25.
17. Suzuki K, Kusumoto M, Watanabe S, et al. Radiologic classification of small adenocarcinoma of the lung: radiologic–pathologic correlation and its prognostic impact. *Ann Thorac Surg* 2006;81:413–9.
18. Gex G, Pralong JA, Combescure C, et al. Diagnostic yield and safety of electromagnetic navigation bronchoscopy for lung nodules: a systematic review and meta-analysis. *Respiration* 2014;87:165–76.
19. Kim TJ, Lee JH, Lee CT, et al. Diagnostic accuracy of CT-guided core biopsy of ground-glass opacity pulmonary lesions. *AJR Am J Roentgenol* 2008;190:234–9.
20. Tay JH, Irving L, Antippa P, et al. Radial probe endobronchial ultrasound: factors influencing visualization field of peripheral pulmonary lesions. *Respirology* 2013;18:185–90.
21. Tamiya M, Okamoto N, Sasada S, et al. Diagnostic yield of combined bronchoscopy and endobronchial ultrasonography, under LungPoint guidance for small peripheral pulmonary lesions. *Respirology* 2013;18:834–39.
22. Sasada S, Izumo T, Chavez C, et al. Blizzard Sign as a specific endobronchial ultrasound image for ground glass opacity: a case report. *Resp Med Case Rep* 2014;12:19–21.
23. Izumo T, Sasada S, Chavez C, et al. The diagnostic utility of endobronchial ultrasonography with a guide sheath and tomosynthesis images for ground glass opacity pulmonary lesions. *J Thoracic Dis* 2013;5:745–50.